Virologica Sinica 40 (2025) 499–502

Contents lists available at ScienceDirect

Virologica Sinica

journal homepage: www.keaipublishing.com/en/journals/virologica-sinica
www.virosin.org

Letter

A mouse model of Crimean-Congo hemorrhagic fever virus-induced coagulopathy

Hui Zhang [a,b], Ziyang Jiang [a,b], Haidang Liao [a,b], Jiang Li [a], Manli Wang [a], Yiwu Zhou [c,*], Zhihong Hu [a,*], Jia Liu [a,*]

[a] State Key Laboratory of Virology and Biosafety, Wuhan Institute of Virology, Center for Biosafety Mega-Science, Chinese Academy of Sciences, Wuhan, 430071, China
[b] University of Chinese Academy of Sciences, Beijing, 100049, China
[c] Department of Forensic Medicine, Tongji Medical College of Huazhong University of Science and Technology, Wuhan, 430030, China

Dear Editor,

Crimean–Congo hemorrhagic fever (CCHF), caused by the CCHF virus (CCHFV), is a severe tick-borne illness with a wide geographical distribution, posing a significant threat with case fatality rates ranging from 5% to 70% (Hawman and Feldmann, 2023). Due to the lack of approved vaccines and therapeutics, the World Health Organization (WHO) has listed CCHF as one of the priority diseases (Semper et al., 2024). CCHF initially presents as a nonspecific febrile illness, characterized by fever, malaise, myalgia, and nausea, which can rapidly progress to hemorrhagic disease. The hemorrhagic stage is particularly pronounced in severe cases, with rapid progression to disseminated intravascular coagulation (DIC), overt bleeding, kidney or liver failure, and shock (Frank et al., 2024). Up to date, there is an absence of a suitable animal model that can accurately mimic the coagulopathy and bleeding associated with CCHFV infection. Consequently, our understanding of the pathogenic mechanisms underlying these conditions remains limited (Rodriguez et al., 2022).

In this study, we employed mice deficient in the signal transducer and activator of transcription 1 (STAT1) protein, a pivotal component in all three interferon signaling pathways, to establish a mouse model of CCHFV-induced coagulopathy. Previously, STAT1$^{-/-}$ mice have been shown to be susceptible to CCHFV infection and the infected mice could develop leukopenia and thrombocytopenia. However, whether they exhibit coagulopathy remains unknown (Bente et al., 2010). We first determined the 50 % lethal dose (LD_{50}) of CCHFV in STAT1$^{-/-}$ mice. Mice were intraperitoneally inoculated with different doses (0.01–1000 $TCID_{50}$) of CCHFV strain YL16070 (Guo et al., 2017), and were monitored daily. Mice exhibiting a weight loss exceeding 10 %, along with two or more symptoms such as ruffled fur, hunched posture, lethargy, curling up, or shaking, were humanely euthanized for sample collection. Mice infected with high doses (1000, 100, and 10 $TCID_{50}$) of CCHFV showed symptoms at 3 days post-infection (d.p.i.), including weight loss (Fig. 1A) and behavioral changes such as ruffled fur or lethargy. By 5 d.p.i., body weight continued to decrease, with a terminal mean weight loss of approximately 15 %, and these mice experienced 100 % mortality (Fig. 1A and B). Mice infected with low doses (1, 0.1, and 0.01 $TCID_{50}$) of CCHFV began to lose weight at 4 d.p.i. and experienced dose-dependent mortality rates. The LD_{50} of CCHFV in STAT1$^{-/-}$ mice was determined to be 0.07 $TCID_{50}$, which is significantly lower than the previously reported LD_{50} (4 PFU) of CCHFV strain IbAr 10,200 in STAT1$^{-/-}$ mice (Bente et al., 2010), this may be related to differences in virus strains and methods of titer determination. The 1000 $TCID_{50}$ dose was used for the following experiments.

Certain clinical markers such as thrombocytopenia, leukopenia, and elevated levels of aspartate aminotransferase (AST), alanine aminotransferase (ALT), and lactate dehydrogenase (LDH) are hallmarks and predictors of fatality of severe CCHF in humans (Bozkurt and Esen, 2021; Frank et al., 2024). Consequently, blood samples were collected at 5 d.p.i. from mice infected with 1000 $TCID_{50}$ of CCHFV for routine blood tests and biochemical analyses. The results revealed a significant decrease in platelet and lymphocyte counts in the peripheral blood of infected mice (Fig. 1C). Moreover, the serum levels of ALT and AST increased dramatically in CCHFV-infected mice compared to those in control mice, indicating severe liver dysfunction induced by CCHFV (Fig. 1C).

Tail bleeding assay was performed at 4 d.p.i. with mice infected with 1000 $TCID_{50}$ of CCHFV and control mice. Infected mice exhibited significantly prolonged tail bleeding times (all exceeding 10 minutes) compared to control mice, suggesting coagulopathy in the infected mice (Fig. 1D). Physiological hemostasis is a complex process involving blood vessels, platelets, coagulation system, anticoagulation system, and fibrinolytic system. Coagulation tests were performed and the results revealed that both prothrombin time (PT) and activated partial thromboplastin time (APTT) were significantly reduced by CCHFV infection at

* Corresponding authors.
E-mail addresses: zhouyiwu@hust.edu.cn (Y. Zhou), huzh@wh.iov.cn (Z. Hu), liujia@wh.iov.cn (J. Liu).

https://doi.org/10.1016/j.virs.2025.04.008
Received 27 January 2025; Accepted 27 April 2025
Available online 30 April 2025

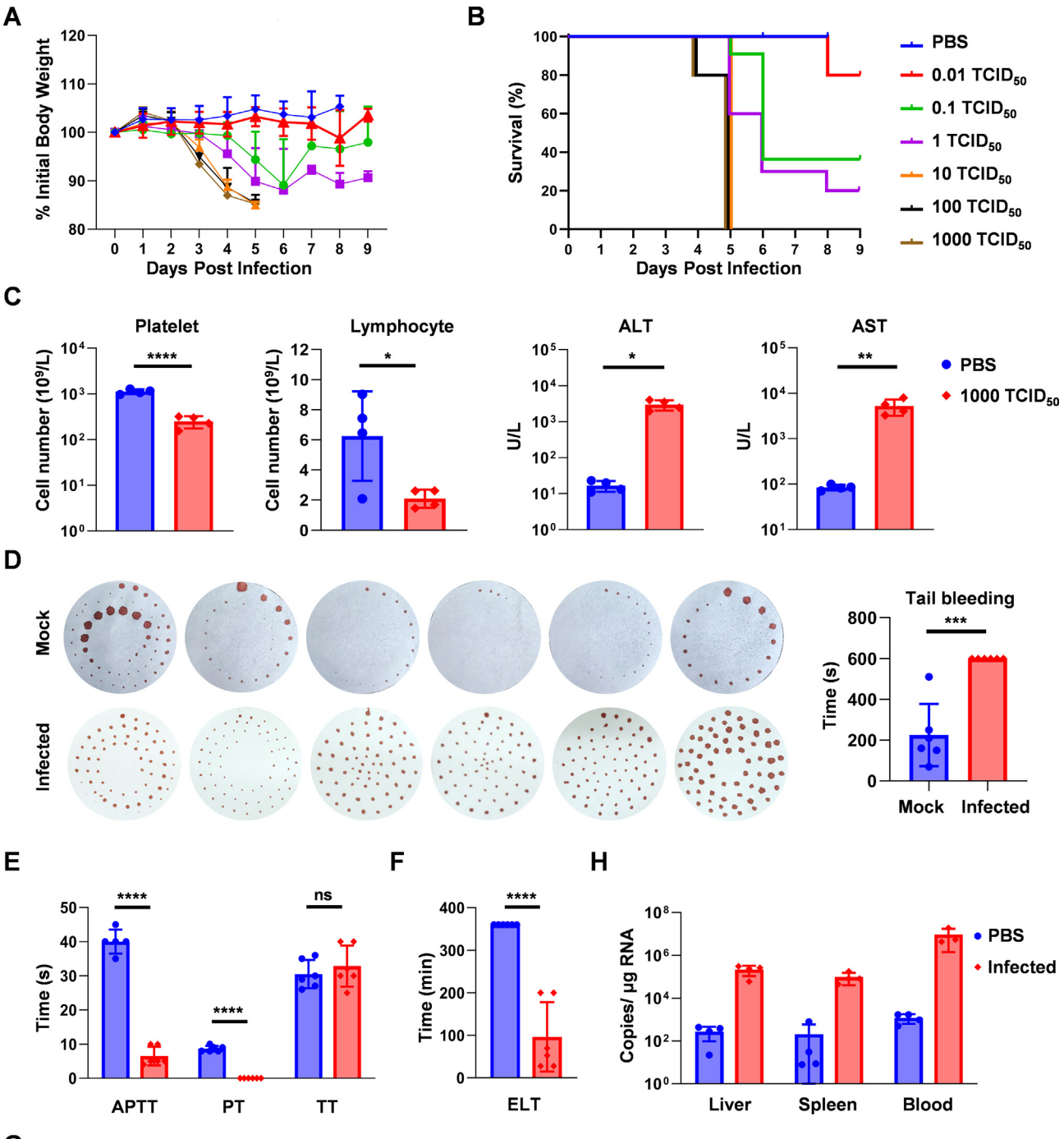

(caption on next page)

Fig. 1. STAT1$^{-/-}$ mice infected with CCHFV exhibited severe pathology. **A, B** Male STAT1$^{-/-}$ C57BL/6J mice of 8 ~ 12-week-old were intraperitoneally inoculated with 0.01–1000 $TCID_{50}$ of CCHFV or mock-infected with PBS. Body weight and behavioral changes of mice were monitored daily. Body weight changes (**A**) and survival rates (**B**) of infected and uninfected mice were monitored daily. **C** Blood samples were collected from control and 1000 $TCID_{50}$ of CCHFV infected mice at 5 d.p.i. The platelet and lymphocyte counts were deteced. The serum levels of alanine aminotransferase (ALT) and aspartate aminotransferase (AST) were analyzed. **D** Tail bleeding time and images of bleeding patterns on filter paper of 1000 $TCID_{50}$ of CCHFV infected mice and control mice were determined at 4 d.p.i. **E** Prothrombin time (PT), activated partial thromboplastin time (APTT), and thrombin time (TT) of control and 1000 $TCID_{50}$ of CCHFV infected mice were measured at 4 d.p.i. **F** Euglobulin clot lysis time (ELT) of control and 1000 $TCID_{50}$ of CCHFV infected mice at 4 d.p.i. **G** Hematoxylin and eosin (H&E) analysis of pathology in the liver, spleen and intestine of control and 1000 $TCID_{50}$ of CCHFV infected mice at 5 d.p.i. White asterisk indicates extensive coagulation necrosis of hepatocytes. Yellow arrows showed small thrombi in blood vessels in the liver and the spleen. Blue arrows showed hemorrhages in intestine. **H** CCHFV S segment copy number in the liver, spleen, and blood of infected mice were detected at 5 d.p.i. The data are presented as the mean ± SD. Statistical significance was determined using student's *t*-test. ns indicates $P > 0.05$. *, **, *** and **** indicate $P < 0.05$, $P < 0.01$, $P < 0.001$, and $P < 0.0001$, respectively.

4 d.p.i., while thrombin time (TT) remained unaffected (Fig. 1E). We further quantified the euglobulin clot lysis time (ELT), which measures the time required to dissolve a clot formed *in vitro* in the euglobulin fraction of plasma in the absence of plasmin inhibitors. As depicted in Fig. 1F, the ELT was significantly diminished in infected mice. Collectively, these data suggest severe coagulopathy in CCHFV infected mice.

Gross inspection of organs from 1000 $TCID_{50}$ CCHFV-infected STAT1$^{-/-}$ mice at 5 d.p.i. revealed discolored liver and spleen, as well as intestinal hyperemia, while organs from mock-infected controls appeared normal (data not shown). Histopathological analysis using hematoxylin and eosin (H&E) staining showed severe pathology in CCHFV-infected mice (Fig. 1G). The liver exhibited extensive coagulation necrosis of hepatocytes (white asterisk), and the spleen showed white pulp atrophy with boundary disappearance. Additionally, small thrombi in blood vessels (yellow arrows) were observed in both the infected liver and spleen. In the intestine, mucosal epithelial cells showed nuclear contraction. Some infected mice also displayed intestinal hemorrhages (blue arrows) (Fig. 1G). Quantitative RT-PCR also revealed CCHFV could efficiently replicate in the spleen and liver, and viremia was also observed at 5 d.p.i. (Fig. 1H).

In our STAT1$^{-/-}$ mouse model of CCHFV infection, mice exhibited prolonged tail bleeding time, indicating a coagulopathy. In prior investigations, it was observed that 30% of CCHF patients exhibited DIC characterized by elevated PT and APTT times (Ozturk et al., 2012; Kaya et al., 2014; Hasanoglu et al., 2016). In studies involving CCHFV-infected mice with interferon α/β receptor knockouts, a notable increase in APTT was documented without a corresponding effect on PT (Zivcec et al., 2013). However, in our STAT1$^{-/-}$ mouse model of CCHFV infection, dying mice displayed shortened PT and APTT, suggesting thrombin activation, which was confirmed with evidence of thrombosis in the liver and the spleen. Concurrently, the significantly prolonged ELT suggests that these mice were also undergoing hyperfibrinolysis. The dual manifestation of thrombin activation and hyperfibrinolysis closely resembles the fibrinolytic DIC observed in cases of severe trauma (Thrombosis and Hemostasis Group, 2017; Song et al., 2022). It seems that although PT and APTT were shortened, the prevailing factors—decreased platelet counts and hyperfibrinolysis—ultimately resulted in a bleeding tendency. This was evidenced by prolonged tail bleeding time and intestinal hemorrhages in some mice. This highlights the complex and dynamic nature of the coagulopathy induced by CCHFV infection. In the current study, we collected samples at 4 or 5 d.p.i. from mice infected with a high dose of CCHFV (1000 $TCID_{50}$) for analyses. Further research is necessary to determine whether infected mice progress to a consumptive hypocoagulable state, which should involve examining different infection doses and time points.

In conclusion, we have developed and characterized a mouse model for CCHFV-induced coagulopathy. Our results showed that high doses of CCHFV infection in STAT1$^{-/-}$ mice led to reduced platelet counts, delayed tail bleeding time, shortened PT and APTT, and prolonged ELT. Additionally, histopathology showed thrombus formation in the liver and the spleen of the infected mice, as well as intestinal hemorrhages in some mice. Although the underlying mechanisms remain to be elucidated, this model provides a validated small-animal platform that recapitulates key features of fatal human CCHF, offering a valuable tool for investigating the pathogenesis of CCHFV-induced coagulopathy and hemorrhage.

FOOTNOTES

We thank Jia Wu, Jun Liu, Hao Tang, and Tao Du from BSL-3 Laboratory; Xuefang An, Fan Zhang, He Zhao, Li Li, and Yuzhou Xiao from the animal center of Wuhan Institute of Virology, CAS for their critical support. This work was supported in part by grants from the Strategic Priority Research Program of the Chinese Academy of Sciences (XDB0490000 to Z.H.), National Key Research and Development Program (2021YFF0702002 to J.L., 2022YFC2303300 to Z.H., and 2023YFC2305900 to M.W.), "Youth Commando" project (2023QNTJ-02 TO J.L.) and Key Project (2024JZZD-02 to Z.H.) of State Key Laboratory of Virology and Biosafety, Wuhan Institute of Virology, the National Natural Science Foundation of China (U22A20336 to Z.H. and Y.Z.), and Wuhan Natural Science Foundation (202404071010067 to M.W. and 202404071010068 to J.L.). All animal experimental protocols were evaluated and approved by the Institutional Animal Care and Use Committee of the Wuhan Institute of Virology (WIVAF01202301). All methods were carried out in accordance with relevant guidelines and regulations. The authors declare that they have no conflict of interest. Prof. Manli Wang is an editorial board member for *Virologica Sinica* and was not involved in the editorial review or the decision to publish this article.

Supplementary data to this article can be found online at https://doi.org/10.1016/j.virs.2025.04.008

REFERENCES

Bente, D.A., Alimonti, J.B., Shieh, W.J., Camus, G., Ströher, U., Zaki, S., Jones, S.M., 2010. Pathogenesis and immune response of Crimean-Congo hemorrhagic fever virus in a STAT-1 knockout mouse model. J. Virol. 84, 11089–11100.

Bozkurt, I., Esen, S., 2021. Association between severity grading score and acute phase reactants in patients with crimean Congo hemorrhagic fever. Pathog. Glob. Health 115, 496–498.

Frank, M.G., Weaver, G., Raabe, V., 2024. Crimean-Congo hemorrhagic fever virus for clinicians-epidemiology, clinical manifestations, and prevention. Emerg. Infect. Dis. 30, 854–863.

Guo, R., Shen, S., Zhang, Y., Shi, J., Su, Z., Liu, D., Liu, J., Yang, J., Wang, Q., Hu, Z., Zhang, Y., Deng, F., 2017. A new strain of Crimean-Congo hemorrhagic fever virus isolated from Xinjiang, China. Virol. Sin. 32, 80–88.

Hasanoglu, I., Guner, R., Carhan, A., Kocak Tufan, Z., Yagci-Caglayik, D., Guven, T., Yilmaz, G.R., Tasyaran, M.A., 2016. Crucial parameter of the outcome in Crimean Congo hemorrhagic fever: viral load. J. Clin. Virol. 75, 42–46.

Hawman, D.W., Feldmann, H., 2023. Crimean-Congo haemorrhagic fever virus. Nat. Rev. Microbiol. 21, 463–477.

Kaya, S., Elaldi, N., Kubar, A., Gursoy, N., Yilmaz, M., Karakus, G., Gunes, T., Polat, Z., Gozel, M.G., Engin, A., Dokmetas, I., Bakir, M., Yilmaz, N., Sencan, M., 2014. Sequential determination of serum viral titers, virus-specific IgG antibodies, and TNF-α, IL-6, IL-10, and IFN-γ levels in patients with Crimean-Congo hemorrhagic fever. BMC Infect. Dis. 14, 416.

Ozturk, B., Tutuncu, E., Kuscu, F., Gurbuz, Y., Sencan, I., Tuzun, H., 2012. Evaluation of factors predictive of the prognosis in Crimean-Congo hemorrhagic fever: new suggestions. Int. J. Infect. Dis. 16, e89–93.

Rodriguez, S.E., Hawman, D.W., Sorvillo, T.E., O'neal, T.J., Bird, B.H., Rodriguez, L.L., Bergeron, É., Nichol, S.T., Montgomery, J.M., Spiropoulou, C.F., Spengler, J.R., 2022. Immunobiology of Crimean-Congo hemorrhagic fever. Antivir. Res. 199, 105244.

Semper, A.E., Olver, J., Warner, J., Cehovin, A., Fay, P.C., Hart, P.J., Golding, J.P., Benassi, V., Preziosi, M.P., Al-Asadi, K.H.R., Blumberg, L.H., De La Fuente, J., Elaldi, N., Fletcher, T., Formenty, P.B.H., Gouya, M.M., Günther, S., Hewson, R.,

Jamil, B., Kobinger, G., Korukluoglu, G., Lempereur, L., Palacios, G., Papa, A., Pshenichnaya, N., Schmaljohn, C., Sow, S.O., Sprong, H., Vatansever, Z., Brooks, T.J.G., 2024. Research and product development for Crimean-Congo haemorrhagic fever: priorities for 2024-30. Lancet Infect. Dis. 24, 00656-x.

Song, J.C., Zhang, W., Zhang, L., Yang, J., Zhang, J.H., Zhou, J., Wang, Q.S., Li, W.Q., 2022. Consensus of Chinese experts on standardized evaluation of coagulation dysfunction in severe patients. Med J Chin PLA 47, 107–117.

Thrombosis and Hemostasis Group, Hematology Society of Chinese Medical Association, 2017. Consensus of Chinese experts on diagnosis of disseminated intravascular coagulation (version 2017). Chin. J. Hematol. 38, 361–363.

Zivcec, M., Safronetz, D., Scott, D., Robertson, S., Ebihara, H., Feldmann, H., 2013. Lethal Crimean-Congo hemorrhagic fever virus infection in interferon α/β receptor knockout mice is associated with high viral loads, proinflammatory responses, and coagulopathy. J. Infect. Dis. 207, 1909–1921.